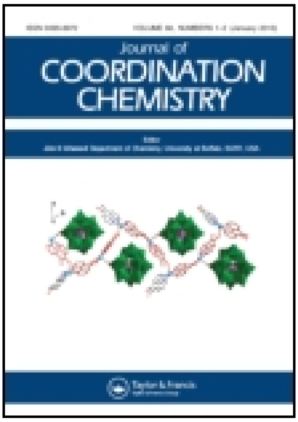

Journal of Coordination Chemistry
Publication details, including instructions for authors and subscription information:
http://www.tandfonline.com/loi/gcoo20

Hydrothermal synthesis, crystal structures, and photoluminescent properties of two cadmium(II) coordination polymers derived from dicarboxylates and N-donor ligands

Jiakun Xu [a] [b] , Xiaochun Sun [c] , Caixia Ju [a] [d] , Lirong Yang [e] , Caifeng Bi [b] & Mi Sun [a]

[a] Yellow Sea Fisheries Research Institute, Chinese Academy of Fishery Sciences , Qingdao , China

[b] Key Laboratory of Marine Chemistry Theory and Technology, Ministry of Education , Ocean University of China , Qingdao , China

[c] National Oceanographic Center , Qingdao , China

[d] College of Food Science and Technology , Shanghai Ocean University , Shanghai , China

[e] College of Chemistry and Chemical Engineering , Henan University , Kaifeng , China

To cite this article: Jiakun Xu , Xiaochun Sun , Caixia Ju , Lirong Yang , Caifeng Bi & Mi Sun (2013) Hydrothermal synthesis, crystal structures, and photoluminescent properties of two cadmium(II) coordination polymers derived from dicarboxylates and N-donor ligands, Journal of Coordination Chemistry, 66:15, 2693-2701, DOI: 10.1080/00958972.2013.813493

To link to this article: http://dx.doi.org/10.1080/00958972.2013.813493

Journal of Coordination Chemistry, 2013
Vol. 66, No. 15, 2693–2701, http://dx.doi.org/10.1080/00958972.2013.813493

Hydrothermal synthesis, crystal structures, and photoluminescent properties of two cadmium(II) coordination polymers derived from dicarboxylates and N-donor ligands

JIAKUN XU*†‡, XIAOCHUN SUN§, CAIXIA JU†¶, LIRONG YANG||, CAIFENG BI‡ and MI SUN*†

†Yellow Sea Fisheries Research Institute, Chinese Academy of Fishery Sciences, Qingdao, China
‡Key Laboratory of Marine Chemistry Theory and Technology, Ministry of Education, Ocean University of China, Qingdao, China
§National Oceanographic Center, Qingdao, China
¶College of Food Science and Technology, Shanghai Ocean University, Shanghai, China
||College of Chemistry and Chemical Engineering, Henan University, Kaifeng, China

(*Received 25 January 2013; in final form 18 April 2013*)

Two metal coordination polymers, $[Cd(ipa)(L_1)(H_2O)]_n$ (**1**) and $[Cd(ipa)(L_2)]_n$ (**2**) [H_2ipa = isophthalic acid, L_1 = 3,5-bis(imidazole-1-yl)pyridine and L_2 = 3,5-bis(benzoimidazo-1-ly)pyridine], have been synthesized and structurally characterized by IR, elemental analysis, XRD, and X-ray single-crystal diffraction. Complex **1** shows a twofold cds topological net and **2** features a 3-D pcu topological net. Luminescent properties of **1** and **2** were investigated in the solid state at room temperature.

Keywords: Cd coordination polymers; Crystal structures; Luminescent properties

1. Introduction

Construction of metal-organic frameworks (MOFs) based on metal ions and organic bridging ligands has attracted attention for intriguing structures and applications in storage [1, 2], luminescence [3, 4], magnetism [5], drug delivery [6], catalysis [7, 8], sensors [9], and separations [10]. The functionalities of MOFs could be designed and fine-tuned through judicious choices of bridging ligands and metal centers. Rigid ligands, such as benzenedicarboxylates, have been utilized to construct MOFs: (a) it can be partially or completely deprotonated to generate H_2ipa, Hipa$^-$ and ipa^{2-} by controlling the pH, which allows H_2ipa to display various acidity-dependent coordination modes. (b) H_2ipa has a rigid 120° angle between the benzene ring and the two carboxylate groups, and therefore may provide various coordination modes to form discrete metal complexes under

---

*Corresponding authors. Email: xujk@ysfri.ac.cn(J.XU); hhsunmi@yeah.net (M. Sun) appropriate synthesis conditions. (c) Flexible, multidentate coordination sites provide the possibility of formation of higher-dimensional structures. Typical coordination modes of H_2ipa are reported [11–14]. Flexible ligands have been employed for the construction of MOFs with special properties and structures [15–17]. Comparatively, far less research has been devoted to semi-rigid ligands. Nevertheless, MOFs based on semi-rigid ligands have received increasing attention owing to slight conformational changes during assembly, making it easy to control the architectures of MOFs [18–21].

SBUs, (3,5-bis(imidazole-1-yl)pyridine) and 3,5-bis(benzoimidazo-1-ly)pyridine, exhibit interesting properties: (i) as semi-rigid bifunctional ligands, they have been employed to construct 1-D and 2-D linear polymeric chains, and therefore are excellent candidates for the construction of supramolecular architectures. (ii) Considering the orientation of pyridine rings, they are effective as targets in the formation of lower dimensional to high-dimensional networks. (iii) The pyridine rings are useful in the formation of hydrogen-bonding and π–π stacking interactions, which are important in assembling high-dimensional networks. We, herein, report two new Cd(II) coordination polymers based on semi-rigid L_1 and L_2 and the rigid dicarboxylate (H_2ipa).

2. Experimental

2.1. *Materials and physical measurements*

All reagents and solvents were commercially available and used as received. Elemental analyses were carried out on a Carlo Erba 1106 full-automatic trace organic elemental analyzer. Fourier-transform infrared spectra (FT-IR) were recorded on a Bruker Tensor-27 FT-IR spectrometer using dry KBr pellets from 400–4000 cm^{-1}. Solid-state fluorescence spectra were recorded on a Hitachi F-4600 equipped with a xenon lamp and a quartz carrier at room temperature. X-ray powder diffraction (XRPD) measurements were performed on a Bruker D8 diffractometer operated at 40 kV and 40 mA using Cu-Kα radiation ($\lambda = 0.15418$ nm).

2.2. *Syntheses*

2.2.1. $[Cd(ipa)(L_1)(H_2O)]_n$ (1). A mixture of $Cd(CH_3COO)_2 \cdot 2H_2O$ (1 mM), H_2ipa (1 mM), L_1 (1 mM), NaOH (2 mM), and deionized water (18 mL) was sealed in a 25 mL Teflon-lined stainless steel vessel and heated at 160 °C for 96 h. After cooling to room temperature, colorless block crystals were obtained and washed with ethanol several times. Elemental Anal. Calcd (%) for $C_{19}H_{15}CdN_5O_5$: C, 45.12; H, 2.99; N, 13.85. Found: C, 45.14; H, 3.00; N, 13.84. IR: 3118 br, 1602 s, 1545 m, 1505 m, 1441 m, 1383 m, 1310 m, 1245 m, 1115 m1, 1067 m, 931 m, 827 m, 725 m.

2.2.2. $[Cd(ipa)(L_2)]_n$ (2). A similar procedure as for **1** was employed to prepare **2** by changing L_1 to L_2 (1 mM). Colorless block crystals of **2** were collected by filtration and washed with ethanol several times. Elemental Anal. Calcd (%) for $C_{27}H_{17}CdN_5O_4$: C, 55.17; H, 2.92; N, 11.91. Found: C, 55.09; H, 2.89; N, 11.93. IR: 1600 s, 1541 s, 1466 m, 1361 m, 910 m, 827 w, 719 m.

2.3. *X-ray crystallography*

Diffraction intensity data of the single crystals of **1** and **2** were collected on a Bruker SMART APEX II CCD diffractometer equipped with graphite-monochromated Mo-$K\alpha$ radiation ($\lambda = 0.71073$ Å) using a ω-scan mode. Empirical absorption correction was applied using SADABS [22]. The structures were solved by direct methods and refined by full-matrix least-squares on F^2 using SHEXL 97 [23]. All non-hydrogen atoms were refined anisotropically. Hydrogens were located by geometric calculations and their positions and thermal parameters were fixed during the structure refinement. The crystallographic data are summarized in table 1 and bond distances and angles in table 2.

3. Results and discussion

3.1. *Description of crystal structures*

3.1.1. $[Cd(ipa)(L_1)(H_2O)]_n$ (1). The structure of **1** is determined by X-ray single crystal diffraction. As shown in figure 1, each Cd(II) is six-coordinate by four oxygens and two nitrogens, showing decahedral geometry. The Cd–O bond distances range from 2.199 to 2.437 Å and the Cd–N distances are 2.305 and 2.320 Å. The coordination environment of the complex is shown in figure 1(a), suggesting that the central Cd(II) bonds to two ipa ligands and two L_1 ligands simultaneously, each ipa ligand and each L_1 connects two Cd (II) ions to form the plane hexagon $Cd_6(ipa)_2(L_1)_4$ with dimension of 21.59×10.42 Å^2. Remarkably, the coplanar $Cd_6(ipa)_2(L_1)_4$ generates a large nanoscale cage which can be considered as consisting of six Cd(II) vertices, four bended L_2 edges, and two bended ipa molecules, as depicted in figure 1(b). Thus, a 3-D framework is prolongated along *a*, *b*, and *c* axes through cage-to-cage connections. One left-handed helical chain (with a pitch of 10.539 Å) running along the *b* axis in the 3-D framework of **1** is observed. The adjacent

Table 1. Crystallographic data and structure refinement summary for **1** and **2**.

Empirical formula	$C_{19}N_5O_5CdH_{15}$	$C_{27}N_5O_4CdH_{17}$
Formula weight	505.76	587.86
Crystal system	Monoclinic	Monoclinic
Space group	*C2/c*	*C2/c*
Unit cell dimensions	$a = 34.966(2)$ Å	$a = 20.876(2)$ Å
	$b = 20.643(1)$ Å	$b = 14.164(1)$ Å
	$c = 26.328(2)$ Å	$c = 20.012(1)$ Å
	$\beta = 126.408(1)°$	$\beta = 128.877(1)°$
Volume (Å^3)	15,294(1)	4607(2)
Z	8	8
Calculated density (mg/mm^3)	1.757	1.695
Independent reflections ($I > 2\sigma(I)$)	13,554	5215
F(000)	8064	2352
θ range for data collection	1.22–25.05	1.81–27.53
Limiting indices	$-41 \leqslant h \leqslant 41$	$-26 \leqslant h \leqslant 25$
	$-20 \leqslant k \leqslant 24$	$-18 \leqslant k \leqslant 13$
	$-31 \leqslant l \leqslant 25$	$-22 \leqslant l \leqslant 21$
Goodness-of-fit on F^2	1.032	1.045
$R_1{}^a, wR_2{}^b$ [$I > 2\sigma$(I)]	$R_1 = 0.0371$, $wR_2 = 0.0784$	$R_1 = 0.0221$, $wR_2 = 0.0582$
$R_1{}^a, wR_2{}^b$ (all data)	$R_1 = 0.0641$, $wR_2 = 0.0930$	$R_1 = 0.0249$, $wR_2 = 0.0600$
Largest diff. peak and hole (e/Å^3)	1.07 and −0.81	0.41 and −0.50

$^a R = \sum(||F_0| - |F_C||)/\sum|F_0|$. $^b wR = [\sum w(|F_0|^2 - |F_C|^2)^2/\sum w(F_0{}^2)]^{1/2}$.

Table 2. Selected bond lengths (Å) and angles (°) for **1** and **2**.

Compound **1**			
Cd(1)–O(1)	2.199(3)	Cd(1)–O(16)	2.401(3)
Cd(1)–O(1W)	2.437(4)	Cd(1)–N(1)	2.305(4)
Cd(1)–O(15)	2.382(4)	Cd(1)–N(3)^a	2.320(4)
N(1)–Cd(1)–N(3)^a	90.18(14)	O(1)–Cd(1)–N(3)^a	126.21(14)
N(1)–Cd(1)–O(15)	97.83(13)	O(1)–Cd(1)–O(15)	83.06(12)
N(1)–Cd(1)–O(16)	85.37(13)	O(1)–Cd(1)–O(16)	137.60(12)
N(1)–Cd(1)–O(1W)	160.76(15)	O(1)–Cd(1)–O(1W)	92.68(16)
N(3)^a–Cd(1)–O(15)	146.14(12)	O(15)–Cd(1)–O(16)	54.70(11)
N(3)^a–Cd(1)–O(16)	93.61(13)	O(15)–Cd(1)–O(1W)	88.47(14)
N(3)^a–Cd(1)–O(1W)	74.95(15)	O(16)–Cd(1)–O(1W)	83.50(15)
O(1)–Cd(1)–N(1)	106.09(14)		
Compound **2**			
Cd(1)–N(1)	2.252(2)	Cd(1)–O(2)	2.207(2)
Cd(1)–N(3)^b	2.443(2)	Cd(1)–O(3)^a	2.325(1)
Cd(1)–O(1)^c	2.387(1)	Cd(1)–O(4)^a	2.376(2)
O(1)^c–Cd(1)–N(3)^e	170.28(5)	O(3)^d–Cd(1)–O(4)^d	55.79(5)
O(2)–Cd(1)–N(1)	116.72(6)	O(4)^d–Cd(1)–N(3)^e	94.84(6)
O(2)–Cd(1)–N(3)^e	86.62(6)	O(4)^d–Cd(1)–O(1)^c	83.54(6)
O(2)–Cd(1)–O(1)^c	102.90(5)	N(1)–Cd(1)–N(3)^e	92.86(6)
O(2)–Cd(1)–O(3)^d	142.28(5)	N(1)–Cd(1)–O(1)^c	84.64(5)
O(2)–Cd(1)–O(4)^d	88.90(5)	N(1)–Cd(1)–O(3)^d	100.20(6)
O(3)^d–Cd(1)–N(3)^e	84.00(5)	N(1)–Cd(1)–O(4)^d	153.65(5)
O(3)^d–Cd(1)–O(1)^c	87.19(5)		

Notes: Symmetry codes for **1**: ^{a}1/2 + *X*, 3/2 − *Y*, 1/2 + *Z*; for **2**: ^{a}−1/2 + *X*, 1/2 − *Y*, −1/2 + Z; ^{b}+ *X*, − *Y*, −1/2 + *Z*; ^{c}3/2 − *X*, 1/2 − *Y*, 1 − *Z*; ^{d}1/2 + *X*, 1/2 − *Y*, 1/2 + *Z*; ^{e}+ *X*, − *Y*, 1/2 + *Z*.

left-handed helical chains entangle reciprocally through ipa and L_1 bridges to give an unprecedented interwoven double helix architecture, see figure 1(c). If the Cd(II) ions and the organic ligands can be viewed as nodes and linkers, the 3-D framework can be simplified as a cds net. Two identical layers penetrate each other in interpenetrating modes to give a twofold interpenetrating network, as illustrated in figure 1(d) and (e).

3.1.2. [Cd(ipa)(L_2)]$_n$ (2). Single-crystal X-ray diffraction analysis reveals that **2** is a 3-D pcu topological net. As shown in figure 2, Cd(II) adopts an octahedral geometry in which four carboxylate oxygens form three different carboxylate ligands and two nitrogens from L_2. In MOF 2, the carboxylates show bis-monodentate (μ_2-$\eta^1:\eta^1$) and bidentate/chelating (μ_1-$\eta^1:\eta^1$) coordination, as shown in figure 2(a). The μ_2-$\eta^1:\eta^1$ carboxylate groups connect Cd(II) ions to form dinuclear units with a Cd–Cd distance of 4.435 Å. In the framework, Cd(II) ions are connected through carboxylic oxygen bridges in μ_2-$\eta^1:\eta^1$ fashion to propagate an infinite 1-D looped ribbon in which two types of rings are alternately arranged in the pattern $(\mathrm{ABAB})_\infty$. A 16-membered ring, A, is comprised of Cd–ipa–Cd–ipa and an 8-membered ring, B, by Cd–CO_2–Cd–CO_2 units, respectively, as depicted in figure 2(b). If the dinuclear Cd(II) and organic ligands can be viewed as nodes and linkers, the 3-D framework can be simplified as a pcu net, see figure 2(c).

3.2. *XRPD analysis and luminescent properties*

Simulated and experimental XRPD patterns of **1** and **2** are shown in figure 3. All the peaks observed in the measured curves approximately match the simulated curves

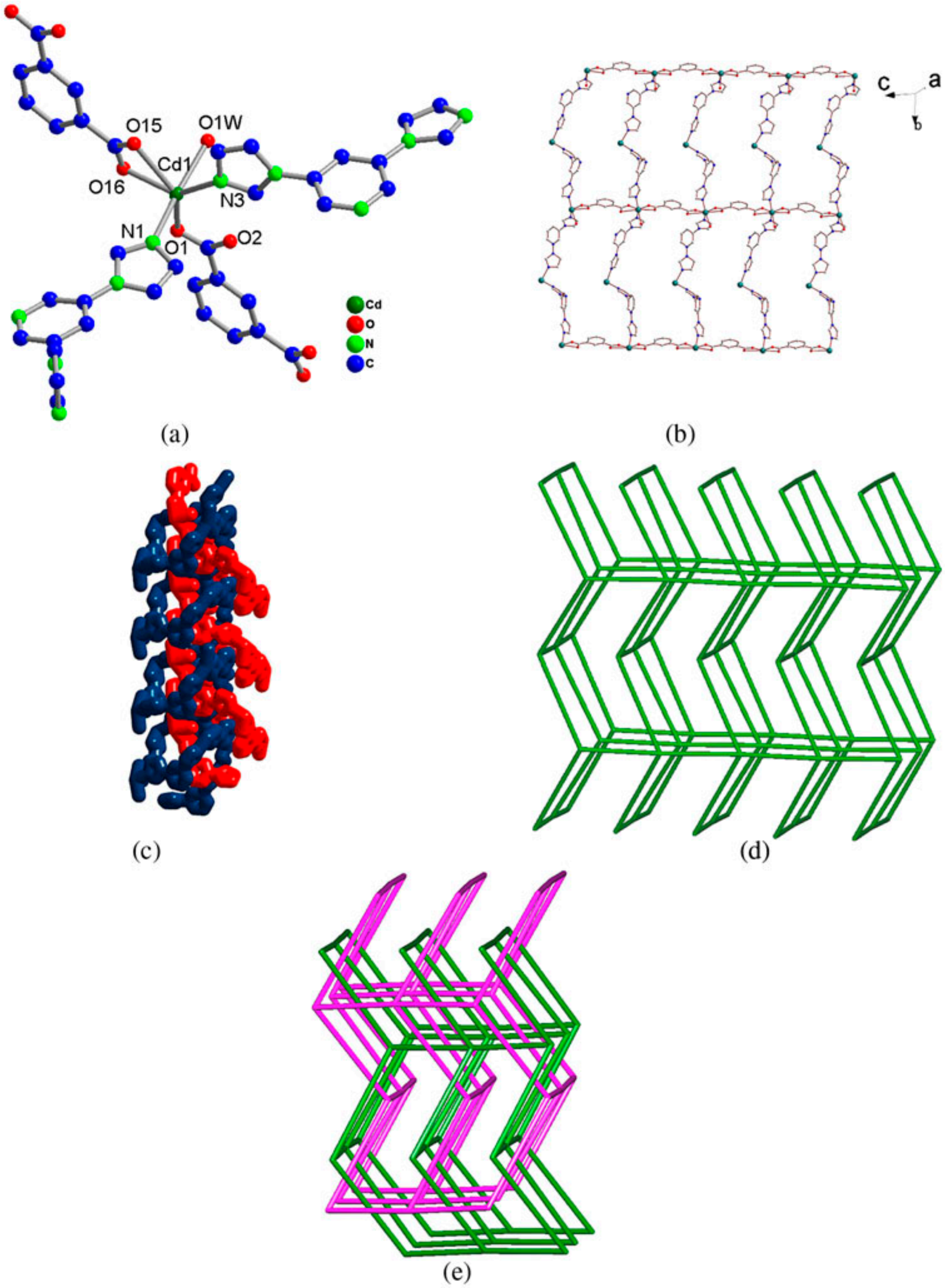

(a) (b) (c) (d) (e)

Figure 1. (a) The coordination environment for Cd(II) in **1**; (b) the coplanar hexagon Cd6(ipa)$_2$(L1)$_4$; (c) the double-stranded helices; (d) the 3-D topological cds net; (e) the twofold interpenetrating cds net of **1**.

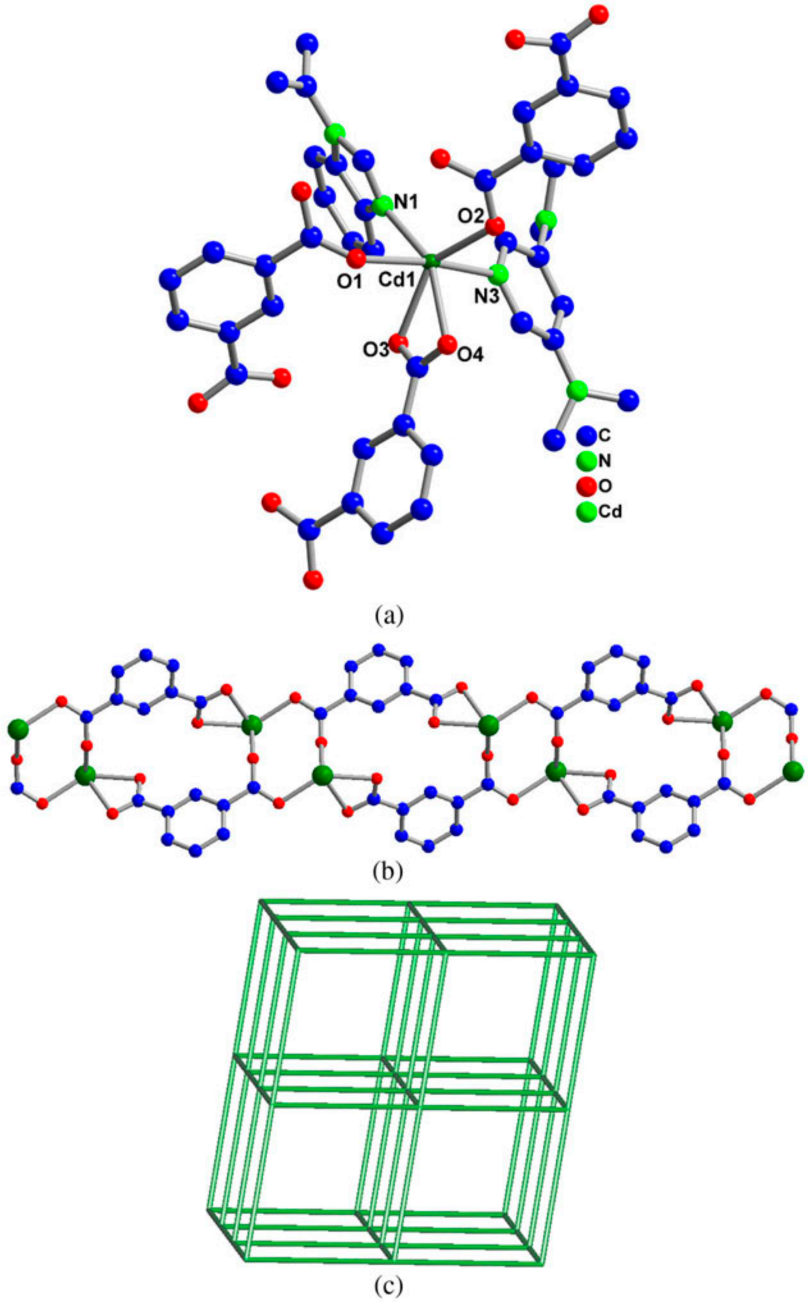

Figure 2. (a) The coordination environment for Cd(II) in **2**; (b) view of 1-D looped ribbon comprising ring A and ring B; (c) diagram of the 3-D pcu net for **2**.

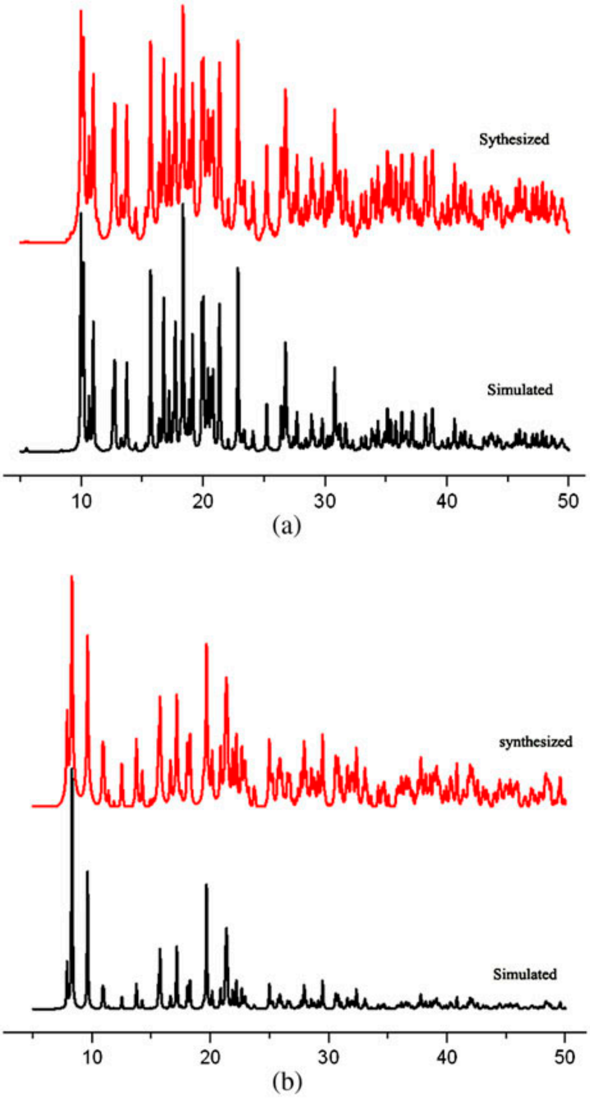

Figure 3. The XRPD for (a) **1**; (b) **2** in the solid state at room temperature.

generated from single-crystal diffraction data, which clearly confirms the phase purity of the as-synthesized products.

Fluorescence emission spectra of **1** and **2** were measured in the solid state at room temperature. Intense luminescence emissions were observed at 408 nm ($\lambda_{ex} = 280$ nm) for **1** and 409 nm ($\lambda_{ex} = 290$ nm) for **2** (figure 4). L_1 and L_2 have an emission band at 411 nm and 352 nm, respectively. The luminous mechanism for **1** and **2** might be intraligand fluorescent emission (π–π^*) [24]. The different emission positions and intensities of **1** and **2** might be attributed to the significant difference in their structures. The ligand coordination to the metal center might contribute to the enhancement of luminescence,

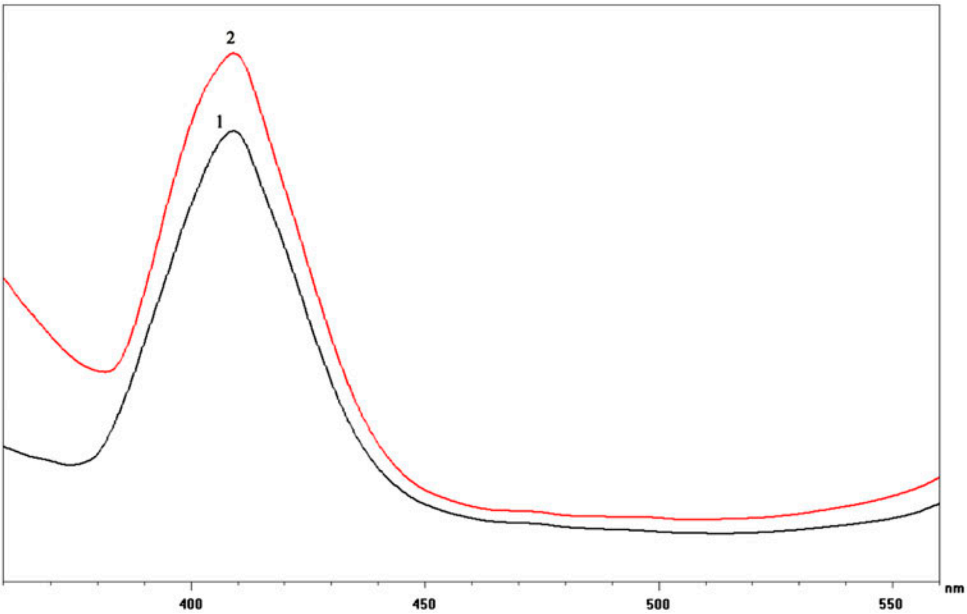

Figure 4. Fluorescence emission spectra for **1** and **2** in the solid state at room temperature.

which effectively increases the asymmetry and rigidity of the ligands, and thereby reduces the non-radiative decay of the intraligand excited state [25].

4. Conclusions

A number of Cd(II) coordination polymers of different network structures have been constructed by utilizing different N-heterocyclic ligands and other auxiliary ligands as the building blocks, most of which coordinate to metal ions in chelating or monodentate fashions [26–34]. Through self-assembly of rigid H_2ipa with Cd(II) in the presence of semi-flexible N-donor ligands L_1 and L_2, we constructed two new coordination polymers $[Cd(ipa)(L_1)(H_2O)]_n$ (**1**) and $[Cd(ipa)(L_2)]_n$ (**2**). Complex **1** shows a twofold cds topological interpenetrating network, while **2** features a 3-D pcu topological net, as reported [33]. The ligand exhibits remarkable versatility to link metals in different coordination modes, which could affect the architecture of the coordination polymers and form different topological frameworks. Moreover, **1** and **2** also exhibit emission in the solid state at room temperature.

Supplementary material

Crystallographic data for the structural analysis have been deposited with the Cambridge Crystallographic Data Center, CCDC reference numbers: 913558 and 913559. These data can be obtained free of charge at http://www.ccdc.cam.ac.uk (or Cambridge Crystallographic Data Center, 12 Union Road, Cambridge CB2 1EZ, UK (Fax: +44 1223 336 033; E-mail: deposit@ccdc.cam.ac.uk).

Acknowledgments

We thank the support of this work by NSFC (Nos. 31200642 and 41106146), Special Funds for the Basic R&D Program in the Central Non-profit Research Institutes (No. 20603022012018), Special Scientific Research Funds for Central Non-profit Institutes, Chinese Academy of Fishery Sciences (No. 2013A1002) and Qingdao Municipal Science, and Technology Plan Project (No. 12-1-4-12-(2)-jch).

References

[1] O.K. Farha, O. Yazaydın, I. Eryazici, C. Malliakas, B. Hauser, M.G. Kanatzidis, S.T. Nguyen, R.Q. Snurr, J. T. Hupp. *Nat. Chem.*, **2**, 944 (2010).
[2] R. Poloni, B. Smit, J.B. Neaton. *J. Am. Chem. Soc.*, **134**, 6714 (2012).
[3] J. An, C.M. Shade, D.A. Chengelis-Czegan, S.P. Petoud, N.L. Rosi. *J. Am. Chem. Soc.*, **133**, 1220 (2011).
[4] G.L. Xu, F. Guo. *J. Solid State Chem.*, **27**, 146 (2013).
[5] L.F. Ma, M.L. Han, J.H. Qin, L.Y. Wang, M. Du. *Inorg. Chem.*, **51**, 9431 (2012).
[6] R.C. Huxford, J.D. Rocca, W. Lin. *Curr. Opin. Chem. Biol.*, **14**, 262 (2010).
[7] M.B. Lalonde, O.K. Farha, K.A. Scheidt, J.T. Hupp. *ACS Catal.*, **2**, 1550 (2012).
[8] P.Y. Wu, C. He, J. Wang, X.J. Peng, X.Z. Li, Y.L. An, C.Y. Duan. *J. Am. Chem. Soc.*, **134**, 14991 (2012).
[9] G. Lu, J.T. Hupp. *J. Am. Chem. Soc.*, **132**, 7832 (2010).
[10] J.R. Li, J. Sculley, H.C. Zhou. *Chem. Rev.*, **112**, 869 (2012).
[11] Y.N. Guo, Y.T. Li, B. Zhi, D.J. Zhang, Y.L. Liu, Q.S. Huo. *RSC Adv.*, **2**, 5424 (2012).
[12] X. Xiao, D.F. Du, M. Tian, X. Han, J.W. Liang, D.S. Zhu, L. Xu. *J. Organomet. Chem.*, **715**, 54 (2012).
[13] R.R. Willis, J.J. Low, S.A. Faheem, A.I. Benin, R.Q. Snurr, A.O. Yazaydin. Gas Adsorption on Metal-organic Frameworks, U.S. Patent No.: 2012.8227375B2.
[14] X.Q. Li, H.B. Zhang, S.T. Wu, J.D. Lin, P. Lin, Z.H. Li, S.W. Du. *CrystEngComm*, **14**, 936 (2012).
[15] T.F. Liu, J. Lu, R. Cao. *CrystEngComm.*, **12**, 660 (2010).
[16] T.F. Liu, J. Lu, R. Cao. *Chem. Commun.*, **46**, 8439 (2010).
[17] P.P. Cui, J.L. Wu, X.L. Zhao, D. Sun, L.L. Zhang, J. Guo, D.F. Sun. *Cryst. Growth Des.*, **11**, 5182 (2011).
[18] X.L. Wang, B. Mu, H.Y. Lin, S. Yang, G.C. Liu, A.X. Tian, J.W. Zhang. *Dalton Trans.*, **41**, 11074 (2012).
[19] J.Y. Lee, C.Y. Chen, H.M. Lee, E. Passaglia, F. Vizza, W. Oberhauser. *Cryst. Growth Des.*, **11**, 1230 (2011).
[20] G.Z. Liu, J.G. Wang, L.Y. Wang. *CrystEngComm.*, **14**, 951 (2012).
[21] Y.L. Wang, J.H. Fu, Y.L. Jiang, Y. Fu, W.L. Xiong, Q.Y. Liu. *CrystEngComm.*, **14**, 7245 (2012).
[22] Bruker AXS. *SAINT Software Reference Manual*, Madison, WI (1998).
[23] G.M. Sheldrick. *SHELXTL NT* (*Version 5.1*), *Program for Solution and Refinement of Crystal Structures*, University of Göttingen, Germany (1997).
[24] X.L. Sun, Z.J. Wang, S.Q. Zang, W.C. Song, C.X. Du. *Cryst. Growth Des.*, **12**, 4431 (2012).
[25] W. Chen, J.Y. Wang, C. Chen, Q. Yue, H.M. Yuan, J.S. Chen, S.N. Wang. *Inorg. Chem.*, **42**, 944 (2003).
[26] L.N. Yang, Y.X. Zhi, J.H. Hei, J. Li, F.X. Zhang, S.Y. Gao. *J. Coord. Chem.*, **64**, 2912 (2011).
[27] D. Zhao, Y. Xiu, X.L. Zhou, X.R. Meng. *J. Coord. Chem.*, **65**, 112 (2012).
[28] C.H. He, C.H. Jiao, J.C. Geng, G.H. Cui. *J. Coord. Chem.*, **65**, 2294 (2012).
[29] C.H. Jiao, C.H. He, J.C. Geng, G.H. Cui. *J. Coord. Chem.*, **65**, 2852 (2012).
[30] T. Li, Y. Xiu, X. Su, X.R. Meng. *J. Coord. Chem.*, **65**, 3111 (2012).
[31] B.F. Huang, H. Huang, H.P. Xiao, J.G. Wang, X.H. Li, A. Morsali. *J. Coord. Chem.*, **65**, 3605 (2012).
[32] D.S. Chowdhuri, S.K. Jana, D. Hazari, M. Bera, A. Rana, E. Zangrando, S. Dalai. *J. Coord. Chem.*, **65**, 3960 (2012).
[33] F. Guo. *J. Coord. Chem.*, **65**, 4005 (2012).
[34] C. Hou, Y. Zhao, T.A. Okamura, P. Wang, W.Y. Sun. *J. Coord. Chem.*, **65**, 4409 (2012).